ACS OMEGA

Open Access

http://pubs.acs.org/journal/acsodf

Article

Preparation of Cellulose Nanocrystals Biofilm from Coconut Coir as an Alternative Source of Food Packaging Material

Md. Hafizul Islam, Mosummath Hosna Ara,* Mubarak A. Khan, Jannatul Naime, Md. Abu Rayhan Khan, Md. Latifur Rahman, and Tania Akter Ruhane

Cite This: *ACS Omega* 2025, 10, 8960−8970

Read Online

ACCESS | Metrics & More | Article Recommendations | Supporting Information

ABSTRACT: The current perspective emphasizes on the synthesis of a biofilm from cellulose nanocrystals (CNC) of coconut coir for the development of sustainable packaging materials as an alternative source of plastic. The biofilm was prepared by a solvent-casting method and investigated by various analytical techniques. Of them, surface morphology was observed by SEM, suggesting a crystalline rod shape with particle size of 104−318 nm and diameter of 15−70 nm. However, CNC was incorporated with starch at various ratios ranging from 10:0 to 1:9; the ratio 6:4 of CNC and the binder maximized the mechanical properties of the polymer. In the presence of a plasticizer and a cross-linker, the film possessed high tensile strength (38.4 ± 1.57 MPa) and elongation (8.2 ± 0.39%) compared to commercially available polyethylene (9.84 ± 0.32 MPa and 23 ± 0.74%). The biofilm possessed a great extent of cross-link structure, divulging through the change of contact angle (92°), surface morphology (rough surface), crystallinity (45.36%), water vapor transmission rate (427 g/m^2/day), and thermal stability from 232 to 258 °C. The degree of deterioration was assessed by the soil burial test (30−45 days), highlighting the environmental compatibility of the film.

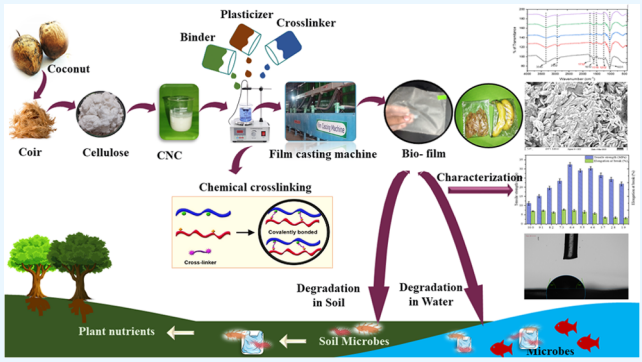

1. INTRODUCTION

The usage of petroleum-based products over the last five decades has created an impact on earth that is irreplaceable and unrecoverable. Scientists and researchers are thriving for alternative biobased sustainable resources to replace petroleum-based packaging materials.[1] One such alternative packaging material is a natural fiber that is biobased, recyclable, and biodegradable material made of cellulose. Moreover, it is a highly suitable material for addressing sustainable and eco-friendly packaging issues, as well as it can reduce the reliance on fossil fuels and diminish greenhouse gas emissions.[2,3]

Cellulose from green sources is the world's inexhaustible and renewable resource with an annual production of about 1.5 × 10^{12} tons and has been widely developed for packaging, mulching film, biomaterials, and other applications.[4,5] Furthermore, cellulose-based films are frequently utilized in packaging films because of their many advantageous qualities, which are predicted to displace PE films derived from fossil fuels. These qualities include renewability, biocompatibility, and environmental friendliness.[4,6] Nanocellulose (NC), which has a diameter of no more than 100 nm, is produced by a number of methods, including chemical and mechanical treatments as well as enzymatic hydrolysis, after cellulose has been extracted from raw materials.[7] Cellulose nanocrystals (CNC) are one of the interesting materials that have attracted many researchers over the decades as they exhibit a number of characteristics that indicate promising applications in the fields of biomedicine, materials packaging, papermaking, and other fields. These features include high Young's modulus, high crystallinity, high specific surface area, and high tensile strength.[7]

Cellulose and its derivatives can be blended with various biopolymer matrices such as starch and polylactic acid (PLA) to improve their physical and mechanical qualities.[8] Again, the products made from natural polymers are stiff and brittle; thus, it is required to add a plasticizer to the polymer matrix to enhance their flexibility properties. Glycerol is one of the plasticizers utilized in the production of packaging materials that has scientific impact because of its low cost and high availability.[9] Moreover, the mechanical properties of a material can be enhanced by using cross-linking agents, such as citric acid, boric acid, glutaraldehyde etc.[10] Fruits frequently contain citric acid (CA), which is a cheap and easily accessible organic

Received: July 10, 2024
Revised: December 30, 2024
Accepted: January 13, 2025
Published: February 27, 2025

Table 1. Experimental Design for Biofilm Preparation (Optimization of CNC, Starch, Glycerol, and Citric Acid)

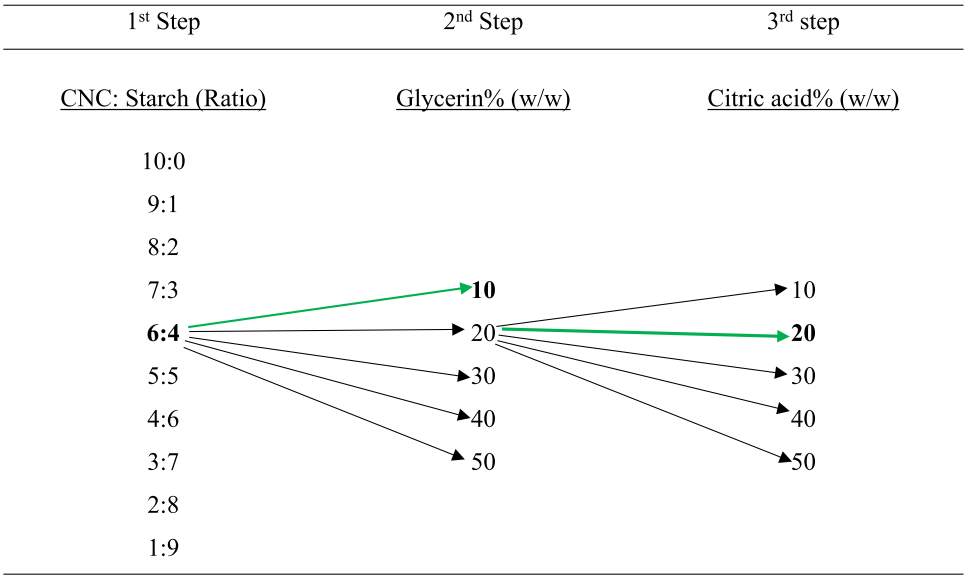

acid. The multicarboxylic structure of CA can create more covalent bonds to the existing hydrogen bonds, enhancing the water resistance and increasing the mechanical strength.[11] The most crucial aspect is that both glycerol and CA are nutritionally safe because they are nontoxic metabolic products of the body that have already been approved by the US FDA (Food and Drug Administration) for use in food compositions.[12]

The production of coconut is concentrated in tropical Asian countries, like Indonesia, India, Bangladesh, Sri Lanka, and Vietnam.[13] Bangladesh ranked the 12th position in the world for coconut production, with over 2800 ha of coconut land and an average annual production of 431,596 MT.[14] Coconut fiber, frequently referred as coir fiber, consists of around 3−4% pectin, 0.15−2.5% hemicellulose, 30−46% lignin, and 32−50% cellulose.[15,16] Most of the time, it is composted, burned, or disposed in landfills to create organic fertilizers. Burning coir fiber causes air pollution and other environmental issues.[17]

Due to the growing consumer demand for safe and healthy food products without containing synthetic additives, we aimed to explore a novel, effective, and innovative food preservation technology that can make the food packaging sector an emergent trend area with a great business potential. Therefore, the aim of this research was to extract cellulose from coir fiber and develop an environmentally friendly biofilm as packaging material that will be mechanically strong and robust during service as well as maintain a unique balance between degradability and durability. In this study, a novel experimental design was developed for the preparation of the biofilm. The study also explored the use of glycerol as a plasticizer and CA as a cross-linking agent at different ratios to optimize the preparation of the biofilm. Throughout the research, environment pollution could be reduced and the waste product of coconut could be utilized as a value-added product. Moreover, a variety of advanced characterization techniques were used in this research to investigate the chemical structure, thermal stability, surface morphology, hydrophobic property, mechanical strength, water vapor permeability, and biodegradability of the prepared film.

2. MATERIALS AND METHODS

2.1. Materials. In this research, sulfuric acid (ACS reagent, purity 95.0−98.0%), sodium chlorite (analytical grade, purity 80%), potato starch (Sigma-Aldrich, purity ≥98%), acetic acid (purity ≥99%), and sodium hydroxide (reagent grade, purity ≥98%) were purchased from Sigma-Aldrich for the extraction of cellulose and preparation of CNC. Glycerol as plasticizer (ACS reagent, purity ≥99.5%), and citric acid (analytical grade, purity ≥99.5%) as cross-linking agent were both purchased from Sigma-Aldrich for the preparation of the biofilm.

2.2. Cellulose Extraction and Isolation of CNC. Coconuts belonging to the *Cocos nucifera* species were collected from the local market of Khulna, Bangladesh. The samples were brought to the lab to be chopped, sun-dried, and then cut into small pieces about 3−5 mm long. In this research, cellulose was extracted from coir fiber using alkali treatment and a bleaching process according to a previous method with slight modifications.[18] This chemical treatment method was optimized for the extraction of high cellulose content within a short period of time and utilization of lower energy consumption compared to previous reports.[18−20] Then, 10.0 g of coconut coir was treated with 200 mL of 5, 10, 15, and 20% (w/v) sodium hydroxide aqueous solution and the mixture was stirred constantly at 200 rpm for 4 h at 90 °C. Deionized water was used several times to wash the alkali-treated fiber until the alkali was entirely eliminated. After that, 300 mL of 2% (w/v) sodium chlorite solution was used to execute the bleaching process. In order to keep the solution's pH at 4, acetic acid was added. After 3 h of stirring (250 rpm) at 80 °C, the mixture was cleaned with deionized water until the pH reached neutral. Then, cellulose was oven-dried at 60 °C and the yield of cellulose from the samples was calculated according to eq 1. Finally, cellulose nanocrystals (CNC) were prepared as described in previous studies.[21]

$$\text{cellulose}\ (\%) = \frac{\text{weight of cellulose}}{\text{weight of the sample}} \times 100\% \quad (1)$$

2.3. Preparation of Biofilm. In order to develop the biofilm, CNC was blended with starch in different ratios,

https://doi.org/10.1021/acsomega.4c06400
ACS Omega 2025, 10, 8960−8970

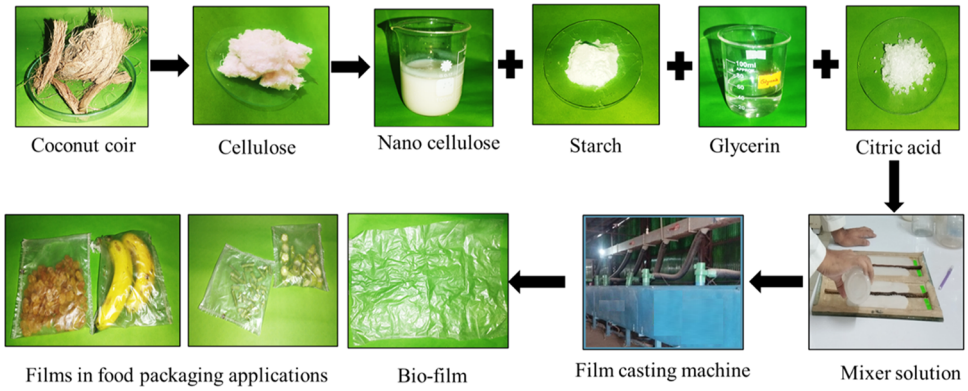

Figure 1. Diagrammatic depiction of the fabrication of the biofilm using CNC, binder (starch), plasticizer (glycerol), and cross-linker (citric acid) as food packaging material.

ranging from 10:0 to 1:9 (Step 1). Then, glycerin was added as the plasticizer, about 10−50% (w/w) by the overall solute weight of CNC and starch (Step 2). Subsequently, CA was added as the cross-linker, about 10−50% (w/w) by the overall solute weight of CNC and starch (Step 3), Table 1. All of the compounds were mixed together by using a high-speed homogenizer (Wiggens D-500 Pro, Germany) until a homogeneous gel-like solution was obtained (stirred at 350 rpm for 30 min, temperature 70 °C). Finally, the films were prepared by the casting method, i.e., casting the prepared suspension on a Polyester Teflon surface and drying it in a film casting machine Figure 1. After each step, the tensile strength and elongation at break were measured by a universal testing machine (UTM). The optimized ratio of CNC to starch (w/w) was 6:4 with glycerol of 10% and CA of 20%. The biofilms were prepared based on the ratio of their mechanical strength for food packaging applications.

The schematic diagram for the preparation of biofilm is given in Figure 1.

2.4. Characterizations. *2.4.1. FT-IR Spectroscopy.* For the identification of functional groups, FT-IR spectra were measured using attenuated total reflectance (ATR) by Shimadzu IRSpirit (Japan). The samples' FT-IR spectra were recorded using an average of 32 scans in the transmittance mode range of 4000−400 cm^{-1}.

2.4.2. Mechanical Tests. A universal testing machine (Zwick Roell Z010, Japan) was used to assess the mechanical characteristics of the produced biofilms, including tensile strength (TS) and elongation at break (Eb%), using the standard test procedure specified by the American Society of Testing and Materials (ASTM D882).[22] With a maximum force capacity of 10 kN, each specimen was evaluated using at least five samples and the testing process was repeated until tensile failure.

2.4.3. X-ray Diffraction (XRD). Crystallographic investigation of the samples was conducted using a Rigaku Smartlab SE (Japan) X-ray diffraction (XRD) machine. The X-ray generator's current and tension was 30 mA and 40 kV, respectively. The wavelength of Cu Kα used was 0.154 nm. The data was acquired throughout the 2θ range, from 4 to 60°, using a step size of 0.02° (2θ) and a scan speed of 0.5°/min. The crystallinity was determined based on the ratio of the crystalline region's area to the total area in the XRD spectra. Equations 2 and 3 was used to compute the crystallinity index and average crystallinity size.[23]

$$\text{crystallinity index, CI (\%)} = \frac{\sum \text{area of crystalline peaks}}{\sum \text{area of crystalline and amorphous peaks}} \times 100\% \quad (2)$$

$$\text{average crystallite size, } D = \frac{K\lambda}{\beta \cos\theta} \quad (3)$$

2.4.4. Scanning Electron Microscopy (SEM). Scanning electron microscopy (SEM) images were analyzed in order to evaluate the surface morphology. The specimens were gold-coated using a sputtering device (JEOL, JFC-1200) with a carbon conductive tape (Ted Pella Inc.) and visualized using ZEISS Sigma 300 VP (Germany) with an accelerating voltage of 15 kV.

2.4.5. Thermogravimetric Analysis (TGA). A thermogravimetric analyzer from the SHIMADZU TGA-50 Series (Japan) was used to examine the thermal characteristics. For each measurement, a platinum pan containing 3−6 mg of the sample was filled. The nitrogen flow rate was maintained at 2 mL/min and thermograms were obtained at temperatures ranging from 30 to 600 °C.

2.4.6. Water Absorption Test. The ASTM D570 standard was followed in determining the water absorption characteristics of the biofilms.[23] Water uptake percentage (%) was calculated using the model (eq 4)

$$\text{water absorption (\%)} = \frac{W_m - W_d}{W_d} \times 100\% \quad (4)$$

where, W_m is the weight of the sample as a function of time and W_d = dry weight.

2.4.7. Water Vapor Transmission Test. The water vapor test was done using textest AG, FX3180 CupMaster, ZURICH (Switzerland), with a slightly modified version of the ASTM E96 test protocol. The parameters were test criterion: equilibrium, weighting interval: 0.50 h, test principle: wet cup, conditioning time: 1 h, solvent: water, test area: 50 cm^2, relative humidity (RH): 80%, velocity: 0.3 m/s, and maximum deviation: 15%. The water vapor transmission rate (WVTR) was calculated according to eq 5

$$\text{WVTR} = \frac{\Delta W}{\Delta t \cdot A} \quad (5)$$

where, $\Delta w/\Delta t$ (g/s) is the flux measured as the weight loss of the cell per unit of time and A (m^2) is the actual exposed area.

https://doi.org/10.1021/acsomega.4c06400
ACS Omega 2025, 10, 8960−8970

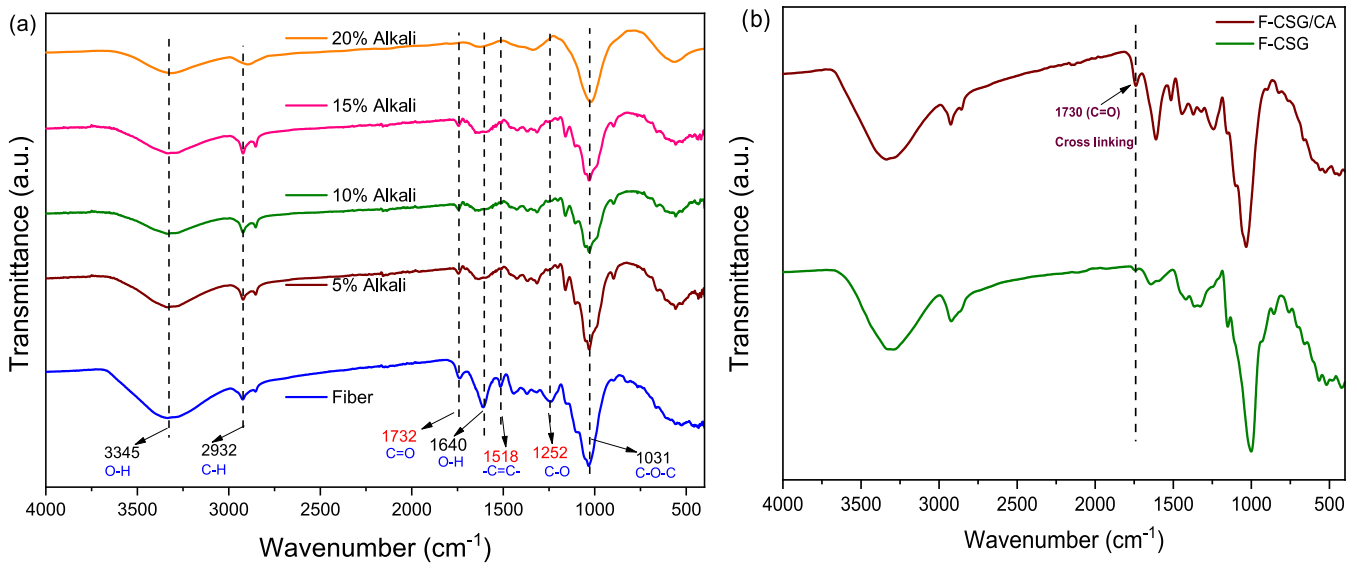

Figure 2. (a) Infrared spectra of coconut coir at different amounts of alkali treatment (5, 10, 15, and 20%); (b) indication of cross-linking in F-CSG/CA by FT-IR spectra (20%), a new peak observed at 1730 cm^{-1} (C═O).

2.4.8. Water Contact Angle. Using the sessile drop method on a Kruss G-1 Contact Angle Goniometer (Germany), the static water contact angle was determined. A strip of the polymer test material was placed on the goniometer testing platform as part of the ASTM D5946 test procedure. Water droplets (3 μL) were dispensed onto the surface using a syringe assembly (30-gauge needle) and images were recorded every 3s.

2.4.9. Soil Burial Test. The soil burial method was used to investigate the biodegradability. For 30 days, the degree of biodegradation was observed. The samples were cut into 4 cm × 4 cm pieces and buried 0.15−0.40 m under the soil.[24] The soil had a neutral pH and a 40% moisture level. After 7, 14, 21, and 30 days, the percentage of deterioration was determined. Before its weight was determined, each sample was taken out, cleaned, and allowed to dry at room temperature. Then, the degree of soil degradation (DSD) was calculated using the following equation (eq 6)

$$\text{degradation in soil (\%)} = \frac{(W_0 - W_d)}{W_0} \times 100\% \quad (6)$$

where, W_0 and W_d are the initial and final dry weight (before and after degradation, respectively).

2.4.10. Statistical Analysis. Each investigation was carried out three times in parallel, and the mean ± standard deviations were used to describe the findings. Using SPSS version 16 software (SPSS, Chicago, IL), all the data were analyzed with no significant difference within the attained values. Analysis of variance (ANOVA) was performed and the significance of each mean property value was determined ($p < 0.05$).

3. RESULTS AND DISCUSSION

3.1. FT-IR Analysis and Composition of Coconut Coir.

After employing 5, 10, 15, and 20% alkali treatment to coir fiber, it was bleached and was assessed using ATR-FT-IR (Figure 2a). The carbonyl (C═O) unconjugated stretching vibration of the ester and the carbonyl group of hemicellulose were responsible for the peak in coconut coir that occurred at around 1740 cm^{-1}, as shown by previous research.[25] The majority of the hemicellulose and pectin were likely removed from the coconut coir in our investigations because the peak at 1732 cm^{-1} disappeared from the FT-IR spectra following 20% alkali treatment. Additionally, it showed that the 5, 10, and 15% alkali treatment was insufficient to eliminate the hemicellulose. The -C═C- stretch of the aromatic rings of lignin is responsible for the characteristic peak at 1520−1510 cm^{-1}.[26] The characteristic peak at 1300−1200 cm^{-1} was induced by C−O out-of-plane stretching of the aryl group of lignin and hemicellulose.[25] The peaks at 1518 and 1252 cm^{-1} could not be observed in cellulose as compared to the native coconut coir. This indicated that the lignin in the coconut coir was effectively removed. Moreover, cellulose treated with different alkalis had identical absorption peaks at around 3400, 2900, 1430, and 1370 cm^{-1}. The absorption peak between 3300 and 3500 cm^{-1} was caused by -OH groups, whereas the peak at 2900 cm^{-1} was attributed to C−H stretching vibrations.[26] The peaks at 1430 and 1370 cm^{-1} were attributed to the C−O−H bending. In the same way, the peaks at 1022, 1313, and 1374 cm^{-1} were related to the C−O−C pyranose ring skeletal vibration, C−C and C−O skeletal vibration, and H-bonded -OH group stretching, respectively, of cellulose.[27,28] In this study, the cellulose content in coconut coir was found to be 39.41 ± 0.72% on a dry weight basis. According to Geethamma et al. and Kongkaew et al., there was 35−43% cellulose in coconut coir, which was consistent with the findings of the current investigation.[29,30]

Moreover, FT-IR spectroscopy analysis is regarded as a valuable tool for the identification of key functional groups and bonding in a compound. Figure 2b illustrates the FT-IR result of the 20% CA content in biofilms. Compared to F-CSG (CNC/starch/glycerin), films with CA denoted by F-CSG/CA (CNC/starch/glycerin/citric acid) exhibit a new band at 1730 cm^{-1}, which may be due to the stretching vibrations of carbonyl groups (C═O), suggesting the existence of carboxylic acid, ketone, or aldehyde compounds formed by the insertion of a cross-linking agent.[31] Since CA contains three carboxylic groups, it is possible that esterification occurred between CA and glycerol, and ester linkage between starch and CNC supports the development of cross-linking.

https://doi.org/10.1021/acsomega.4c06400
ACS Omega 2025, 10, 8960−8970

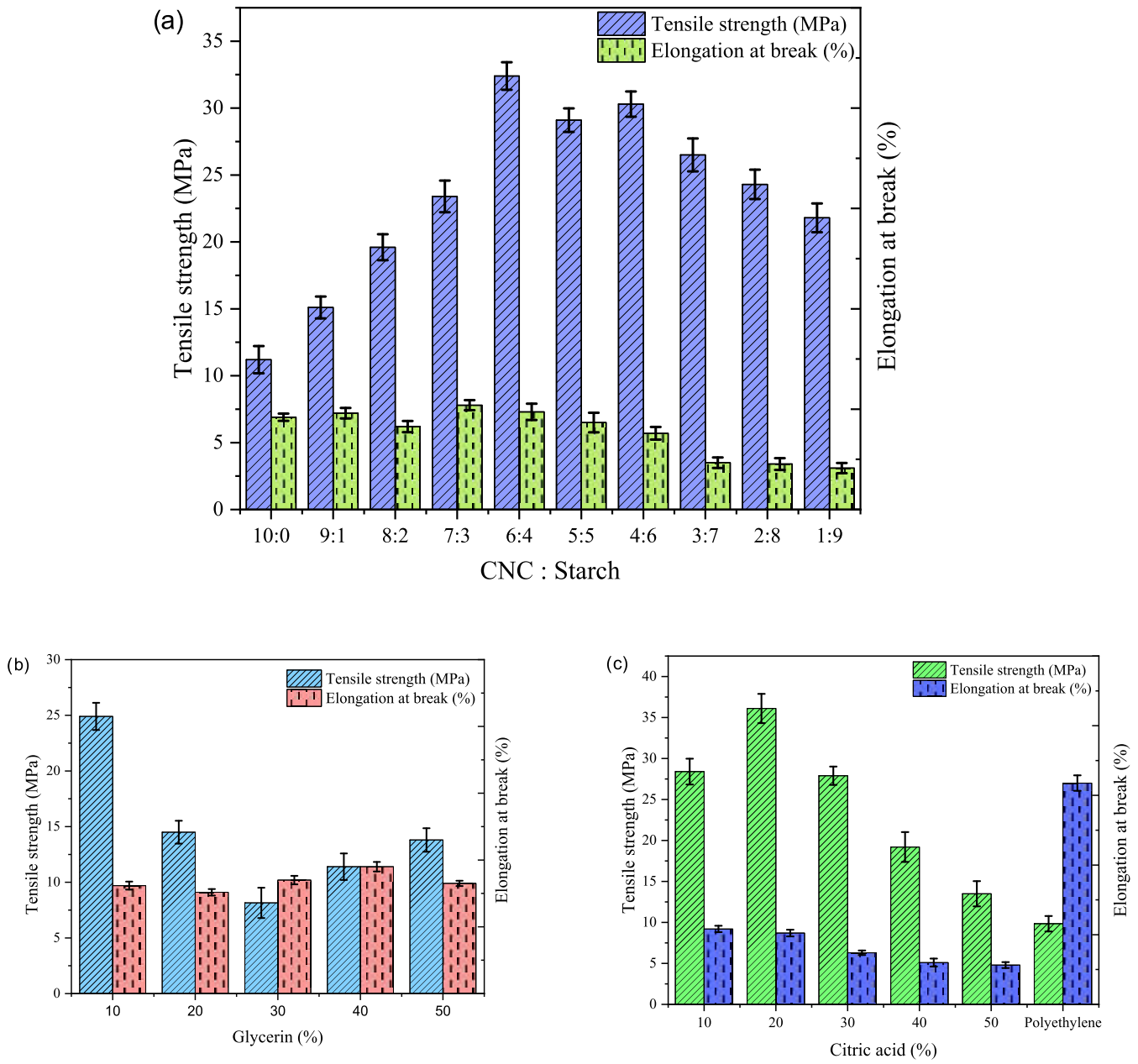

Figure 3. (a) TS and Eb% of CNC: starch biofilm; (b) TS and Eb% of the biofilm at different glycerol contents (10−50%); (c) effect of CA contents (10−50%) on the mechanical properties (TS and Eb%) of biofilms.

The CA that was bonded to CNC and starch has the ability to break down inter- and intramolecular hydrogen bonds.[32]

3.2. Mechanical Properties. The tensile strength (TS) and elongation at break (Eb%) of biofilms at various ratios of CNC, starch, glycerin, and CA are graphically demonstrated in Figure 3. The mechanical properties of CNC/starch (CS)-based biofilms were investigated at different ratios of CNC and starch from 10:0 to 1:9. The TS value of the prepared biofilms ranged from 11.2 ± 1.02 to 32.4 ± 1.03 MPa along with Eb% of 3.1 ± 0.38 to 7.8 ± 0.38%. The F-CS blend polymer showed significant differences in TS with the increase in starch concentrations up to 6:4 ratio and then decreased. The CS ratio (6:4) had the highest TS value of 32.4 ± 1.03 MPa with Eb% of 7.3 ± 0.61%, which could be due to the interfacial interaction between CNC and starch. Consequently, this ratio was recommended for further investigation. Glycerol can increase the flexibility of biofilms by reducing the intermolecular connections between the chains and changing their mechanical characteristics.[22] Glycerol was added to the optimized CS ratio (6:4) at different ratios of the solute weight, ranging from 10 to 50% (w/w). CNC/starch/glycerol (CSG) blend films had TS ranging from 8.15 ± 1.36 to 24.9 ± 1.22 MPa and Eb% of 9.1 ± 0.29 to 11.4 ± 0.43%. The change in elongation was not proportional to the increase in the glycerol content. The elongation of biofilms increased as the glycerol concentrations increased for a certain percentage and then decreased. The optimized glycerol ratio was 10% (w/w) based on mechanical strength, where the TS value was 24.9 ± 1.22 MPa and Eb% was 9.7 ± 0.29%. A higher elongation gives more flexibility, ensuring that it can withstand deformation without fracturing easily. According to many studies, an

https://doi.org/10.1021/acsomega.4c06400
ACS Omega 2025, 10, 8960−8970

increase in glycerol content also enhanced elongation but significantly lowered TS.[31,32]

Finally, cross-linker CA was added to the optimized CSG ratio (6:4−10%) at different ratios of the solute weights ranging from 10 to 50% (w/w). The CNC/starch/glycerol/citric acid (CSG/CA)-based biofilm had TS values ranging from 13.5 ± 1.54 to 38.4 ± 1.57 MPa and Eb% ranging from 8.2 ± 0.39 to 11.8 ± 0.36%. Addition of 20% (w/w) CA into the CSG film gave an optimum value of TS of 38.4 ± 1.57 MPa with an Eb% of 8.2 ± 0.39%. In this study, TS was reduced by adding more CA content. Similarly, Yu et al. reported that the higher the CA content, the more the decrease in TS.[33] Additionally, the researchers observed that CA affects the mechanical performance. A greater concentration of CA can significantly lower the TS while increasing the elongation at break.[34,35] This increase in elongation with the addition of CA might be caused by a synergistic effect, intermolecular interactions between the polymer matrix, and identical polysaccharide structures.[12] Cellulose and starch polymers may develop ester linkages and hydrogen bonds with the hydroxyl and carboxyl groups of CA, which might result in the creation of a robust structure. As a result, mechanical characteristics were enhanced and it can resist the diffusion of water molecules. Therefore, the optimized ratio by mechanical strength for the biofilm was CNC:starch (6:4), glycerin 10%, and CA 20%. The mechanical properties of commercial polyethylene films (plastic polybag) were also investigated by a UTM machine. It had TS 9.84 ± 0.32 MPa with an EB% of 23 ± 0.74%. The TS values of commercial films were lower than those of the optimized biofilm.

3.3. X-ray Diffraction Analysis (XRD). The crystallinity index of coir fibers, cellulose, CNC, F-CSG, and F-CSG/CA was evaluated using the XRD technique (Figure 4). The XRD

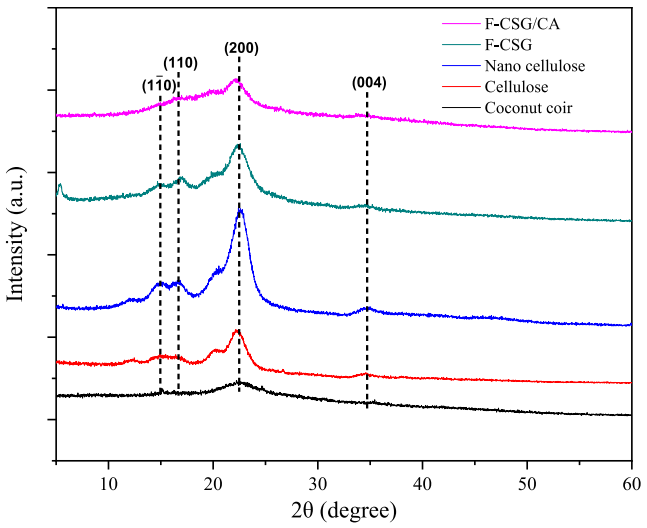

Figure 4. XRD patterns of coconut coir, cellulose, CNC, and the prepared biofilms F-CSG and F-CSG/CA.

patterns of cellulose exhibited the characteristic diffraction peaks around 2θ = 14.6° (110), 16.5° (110), 22.6° (200), and 34.7° (004), as suggested previously, and confirmed that the crystal lattice type I cellulose was formed after chemical treatment.[4,36] The gradually increasing intensity of CNC peaks at 2θ = 16.5 and 22.6° showed that the crystallinity of the material increased by chemical treatment. The CI value increased significantly when transforming from coir fiber (40.27%) into cellulose (63.12%) whereas An et al. found CI 45.4% for coconut husk fiber and 72.7% for pure cellulose.[37] The increase of crystallinity was attributed to the increase of the ordered crystalline region resulted from the ordered cellulose chains.[38] However, the chemical agents, processing technique, and cellulose source have an impact on the CI value.[37] In addition, the average crystallite size of cellulose was 2.89 nm, while the average crystallite size of untreated coir was 6.50 nm. After acid hydrolysis of the coir cellulose, the CI value was 80.59% and average crystallite size was 2.11 nm in CNC due to the removal of amorphous domains of cellulose.[37] The improved CNC rearrangement allows for a highly ordered close packing, which in turn improves the hydrogen interaction between CNC chains to provide the high crystalline and impact structure as well as sharper diffraction peaks.[39]

It was evident that the two biofilm samples had similar characteristic peaks at around 16.5, 22.6, and 34.7°, with a slight variation in intensity. F-CSG/CA showed a much lower crystallinity index (45.36%) than F-CSG (65.28%) because CA disrupted the inter- and intramolecular hydrogen bonds and led to an amorphous polymer structure. Furthermore, the formation of more amorphous cellulose structures in the biofilm was linked to the breakdown of well-organized cellulose microstructures, which in turn caused this shift in crystallinity and was advantageous for flexibility and elongation.[23] Addition of CA in the F-CGS/CA crystallinity index was reduced due to its role in breaking down the cellulose structure. According to Sommer et al., as the concentration of the plasticizer and cross-linker increases, the degree of crystallinity decreases because interactions between the matrix chains become less frequent.[40] However, the actual correlation between the crystallinity and mechanical properties can vary depending on the material and film composition as well as the method of preparation (e.g., annealing, deposition conditions).

3.4. Scanning Electron Microscope (SEM) Analysis. The external morphology (texture) and orientation of materials in the samples were observed by a scanning electron microscope (SEM). Figure 5a shows a comprehensive, enlarged microstructure view of the coir fiber by SEM image. The coir fibers showed a fibrous, string-like appearance with irregular rough surface. In Figure 5b, a collection of closely packed crystalline nanorods can be observed, each with a relatively uniform width but varying lengths. The SEM image revealed the presence of CNC with particle size 104−318 nm and diameter 15−70 nm. The surface of cellulose nanocrystals was smooth with aggregates or clumps.

F-CSG, as shown in Figure 5c, had typically a smooth, compact, orderly surface, which could be clearly observed from the formation of clusters. Glycerin contributed to surface modification, resulting in smoother textures in certain regions due to its moisture-retaining properties. The regions were visible where CNC and starch were more concentrated, forming clusters or aggregates. It also indicated that the addition of glycerin to the samples helped in plasticization and, as a consequence, long chains are formed. The cross-linking by CA influenced the microstructure of the film by surface modification, Figure 5d. CA interacts with CNC, starch, and glycerin, leading to changes in surface roughness and texture. The cross-linking facilitated by CA led to a more interconnected network structure and integrated matrix with uniform arrangement within the film.

https://doi.org/10.1021/acsomega.4c06400
ACS Omega 2025, 10, 8960−8970

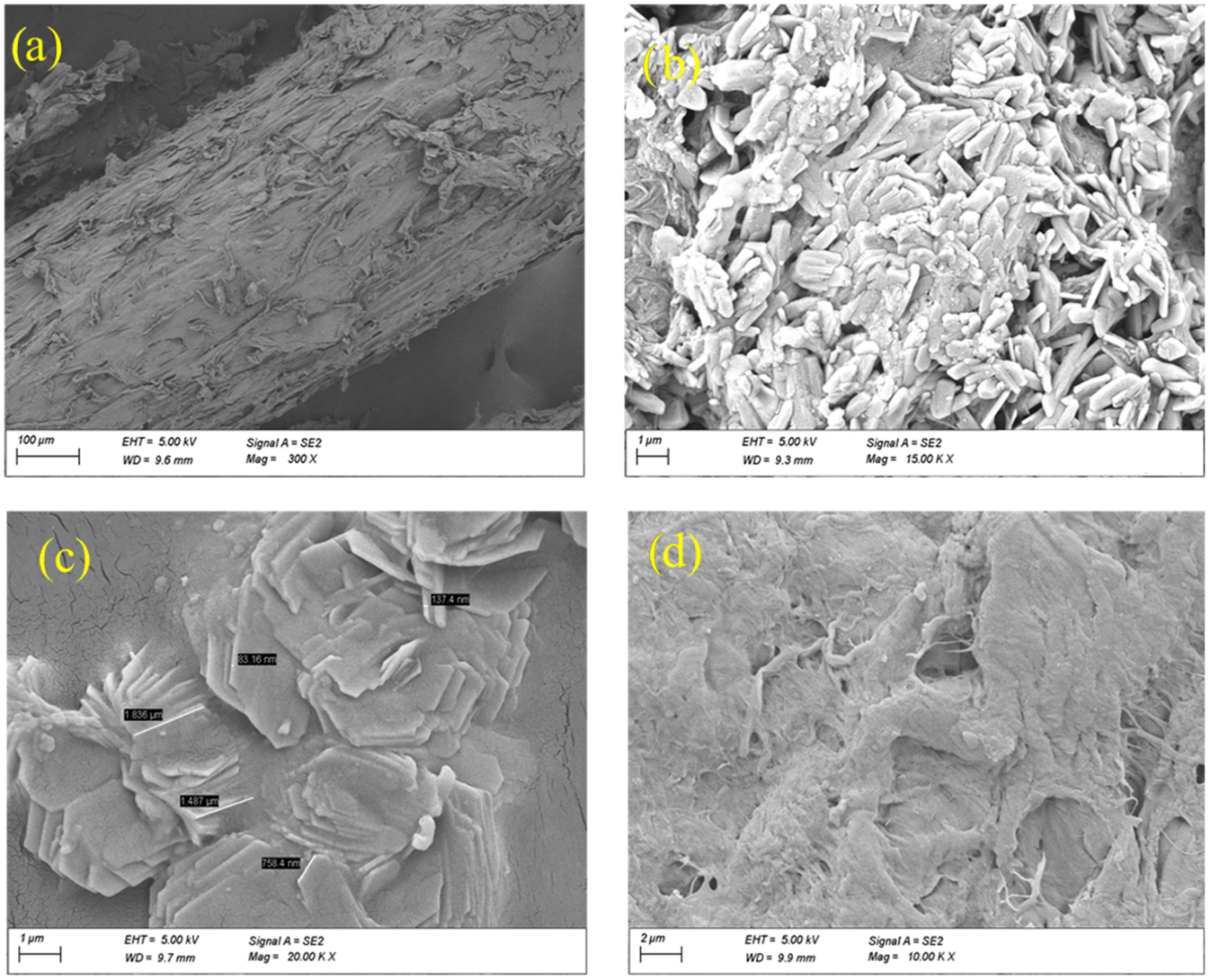

Figure 5. SEM image: (a) coconut coir (scale 100 μm, Mag: 300×); (b) isolated CNC (scale 1 μm, Mag: 15k×); (c) plasticized biofilm F-CSG (scale 1 μm, Mag: 20k×); (d) cross-linked biofilm F-CSG/CA (scale 2 μm, Mag: 10k×).

3.5. Thermogravimetric Analysis (TGA). The TGA curve provides insights into the various stages of decomposition and the associated temperature ranges. According to reports, adding fiber to starch increases its heat stability when there is strong adherence between the fiber and the matrix, which reduces the mass loss in the sample.[41,42] The TG curves of films showed a two-step decomposition pattern, Figure 6. A small weight loss (approximately 8%) was found in the range of 90−110 °C, indicating the evaporation of moisture from the films.

In the F-CSG film, the first predominant stage of degradation started from 232 °C and ended at approximately 353 °C with weight loss 71.47% due to the pyrolysis of starch and CNC (Table 2). Further weight loss in the second degradation was around 413−490 °C (weight loss 97.92%). It was found that the films cross-linked with CA (F-CSG/CA) showed significant thermal stability. The first predominant stage of degradation from 258 to 365 °C (weight loss 57.34%) was primarily due to the degradation of the polymer chain,[43,44] followed by further weight loss in the second degradation region around 426−503 °C (weight loss 93.74%) corresponding to the breakdown of the polymer backbone and

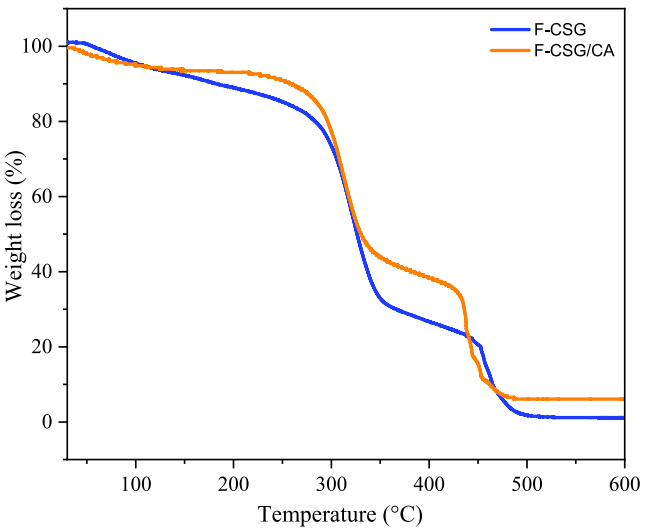

Figure 6. Effect of CA (20%) on the TGA curve of biofilms (F-CSG, F-CSG/CA).

https://doi.org/10.1021/acsomega.4c06400
ACS Omega 2025, 10, 8960−8970

Table 2. Effect of Temperature on Degradation of Biofilms

	1st decomposition region		2nd decomposition region	
composition	temp. (°C)	wt. loss (%)	temp. (°C)	wt. loss (%)
F-CSG	232−353	71.47	413−490	97.92
F-CSG/CA	258−365	57.34	426−503	93.74

degradation of polysaccharide structure (organic fragments).[45] F-CSG/CA had a higher onset temperature (where degradation starts) and a lower mass loss than F-CSG. The improvement in thermal stability confirmed that, with the addition of CA, the adhesion between CNC, glycerol, and starch in the synthesized film was enhanced. CA decreased the intra- and intermolecular interactions between cellulose-cellulose and starch−starch chains and strengthened the bonding interactions between the hydroxyl groups of cellulose and starch.[46]

3.6. Water Absorption and Water Vapor Transmission. CNC and starch are naturally hydrophilic; it was anticipated that the water absorption rate would decrease with CA cross-linking. In this study, the water absorption rates of F-CSG and F-CSG/CA were compared for a time period of 0−120 min. All of the samples had a high absorption rate during the first 10 min of the soaking period, as shown in Figure 7a, and this rate remained constant from 15 to 120 min, which was similar to the previous work of Lee et al.[47] Additionally, Namphonsane et al. conducted a 120 min water absorption test and observed that as the amount of CA increases, the water absorption decreases due to the network of cross-linked structures.[48] A steady increment of water absorption with time was expected until the process reached equilibrium.[49] Because glycerol and starch are hydrophilic, they contributed to the high water absorption in F-CSG.[50] Samples prepared by adding CA as a cross-linker slowed the water absorption rate. Since CA lowered the -OH group by creating an ester bond between CNC and starch, the hydrophilic nature of the biopolymer was diminished, resulting in a lower water absorption.[51] Water resistivity was better in CA samples since they did not break into little fragments during the experiment and kept their forms with just a modest amount of swelling. After 120 min, the F-CSG film showed a significant increment of water absorption percentage (92.41 ± 2.36%) while the F-CSG/CA film showed a lower water absorption percentage (73.13 ± 1.76%). Similar findings have been reported by Gerezgiher et al., who observed that after 2 h, the water absorption (%) of films made from starch, glycerin, and CA was 90−120%.[52] Cross-linking by CA leads to a reduction in free OH groups, which in turn reduces the hydrophilicity and improves water resistance.[53,54] Moreover, chemical and physical bonding were the reasons behind the decreased water absorption property.

Water vapor transmission rate (WVTR) is the most studied property of packaging materials, mainly due to the vital function that water plays in avoiding dehydration and spoiling responses. Figure 7b indicates that F-CSG had water vapor transmission rates of 863 ± 12.52 (g/m^2/day). The values dropped to 427 ± 11.02 (g/m^2/day) after adding CA. The addition of CA led to a significant decrease in water vapor permeability (WVP) for F-CSG/CA, confirming again the formation of a network. WVTR should be as low as feasible since food packaging materials are frequently needed to prevent moisture transfer between food and the environment. Several researchers found that the hydrophilic -OH groups in films were substituted with hydrophobic ester groups upon the addition of CA, resulting in a decrease in WVTR.[12,31] The lower WVTR indicates that oxygen and moisture cannot easily penetrate the packaging material, which is good for food preservation, and food can sustain a long time without spoilage. The WVTR of commercial polyethylene was 59 ± 3.62 (g/m^2/day).

3.7. Water Contact Angle. Water contact angle (WCA) measurement was used to assess the generated biofilm's water resistance performance and to determine whether the films were hydrophobic or hydrophilic in nature. WCA would differ from 0 to 180°, where 0° indicates a highly hydrophilic nature and above 90° indicates a hydrophobic nature.[22] Despite the fact that several researchers have asserted that biomaterial surfaces with a WCA > 65° can be considered as hydrophobic,[55,56] the F-CSG film had a contact angle of 74°, and after addition of CA, the contact angle increased to 92°, suggesting the formation of cross-linking, Figure 8. Moreover, the contact angle of the commercial polyethylene-based plastic

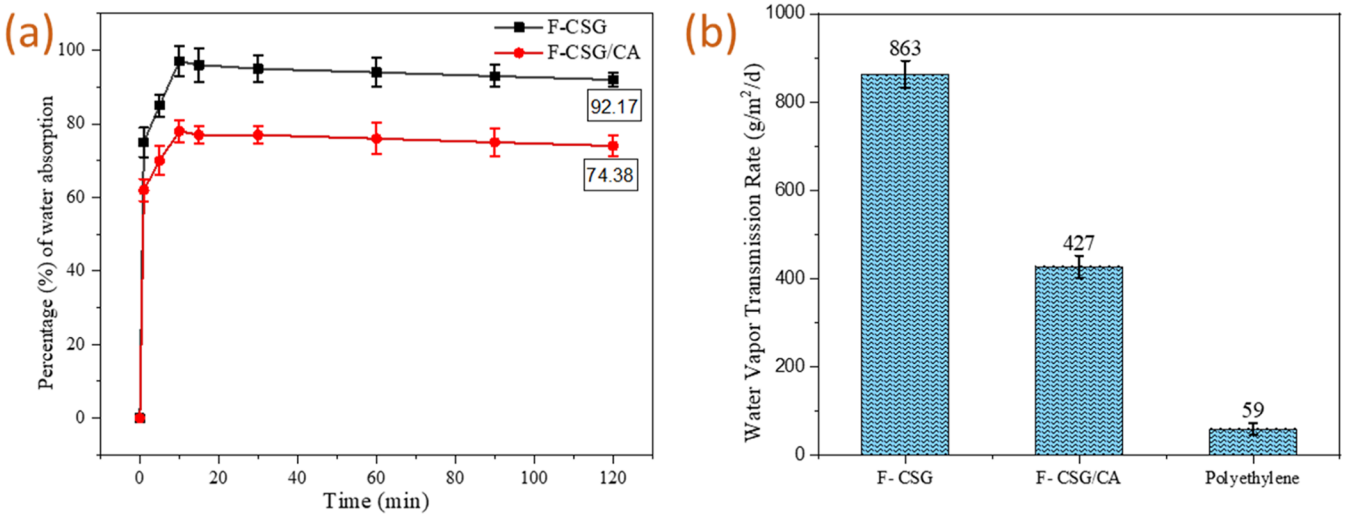

Figure 7. (a) Dependence of water absorption (%) in biofilms (F-CSG, F-CSG/CA) at different storage times and the effect of CA (20%); (b) comparison of the water vapor transmission rates of biofilms (F-CSG, F-CSG/CA) and polystyrene.

https://doi.org/10.1021/acsomega.4c06400
ACS Omega 2025, 10, 8960−8970

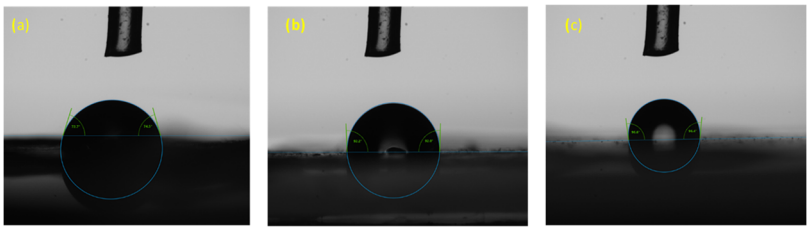

Figure 8. Water contact angle of different films: (a) without cross-linker F-CSG (74°); (b) with cross-linker F-CSG/CA (92°); and (c) commercial polyethylene (96°).

bag was 96°. With a contact angle of 92° and a rougher surface (from SEM), a nanostructure of the F-CSG/CA film contributed to increase the surface hydrophobicity. CA with multicarboxylic structure reacted with the hydroxyl groups of the polysaccharide chain, leading to new chemical bonds and forming a different polymer network. The hydrophilic nature of thermoplastic starch can be diminished by substituting hydroxyl groups with hydrophobic ester groups.[12,57] As a result, it may be claimed that the produced biofilm could be used in a range of consumer goods, including food packaging applications, as well as trash, shopping, and storage bags.

3.8. Soil Burial Test. The biodegradability of the produced biofilms was tested via a soil burial test. All samples lost their weight, demonstrating the process of degradation by microorganisms. After 7 days, films changed their physical appearance and exhibited pores, showing the beginning of degradation. The degradation process of F-CSG film was significant at 7 days, while in the films with CA (F-CSG/CA) 14 days were necessary. After the first 7 days of incubation, there was 17.2 and 11.53% weight loss in F-CSG and F-CSG/CA samples, respectively (Figure 9). After 30 days, the

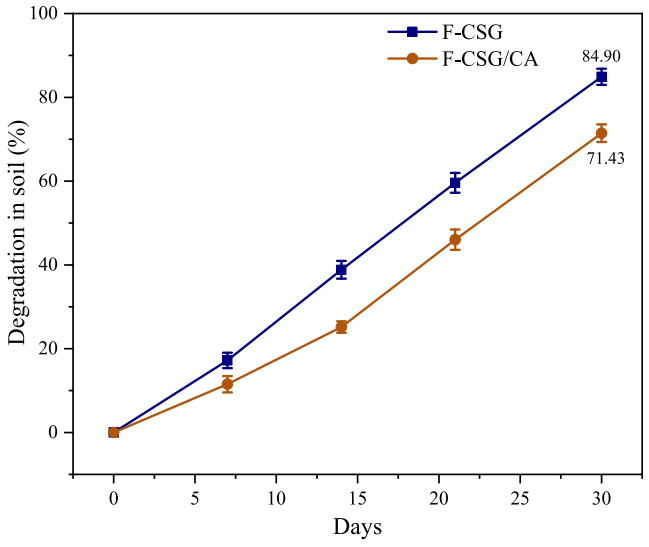

Figure 9. Comparison of degradation in soil (%) of biofilms F-CSG and F-CSG/CA and the effect of CA (20%) in the soil burial test.

percentage of weight loss continued to increase over time and reached 84.90% (F-CSG) and 71.43% (F-CSG/CA), respectively. The experiment suggested that all of the films prepared were biodegradable within 30−45 days. The addition of CA reduced the absorption of moisture; therefore, a decrease in microbial growth in cross-linked samples was anticipated. These results agree with Maiti et al., who observed that cross-linking slowed the biodegradability.[58] Considering that the generation of a network by the use of CA is beneficial to many purposes, it can slow the degradation process.[59] Visual modifications of the samples were also seen after finishing the test. The samples got broken into pieces when touched and micropores were observed, which increased the access sites for water and microorganisms and led to a higher percentage of biodegradation. However, biological activity, moisture content, and temperature may all have an impact on the rate of deterioration.

4. CONCLUSION

The packaging industry plays a significant role in every country's economy because products made in a country need to be packed and transported, which is crucial for the country's overall economy. Currently, packaging materials mainly composed of petroleum-based synthetic polymers face environmental and disposal issues. As a result, developing eco-friendly and biobased polymers as alternatives has motivated academic and industrial research. Coconut coir is a major byproduct that is renewable and recyclable for the preparation of biofilms. In this research, CNC was isolated from coir fiber and the biofilm's durability was enhanced by the addition of a binder, plasticizer, and cross-linker. The optimized ratio of CNC to starch (w/w) was 6:4 with glycerol 10% and CA 20%. In addition, films containing a cross-linker exhibited superior performance in terms of water vapor transmission rate, mechanical characteristics, thermal stability, and contact angle. The developed film possessed a TS of 38.4 MPa with an Eb% of 8.2%, whereas commercially available polystyrene had a TS of 9.8 MPa and an Eb% of 23%. The contact angle of films without CA was 74°; with the addition of CA, the contact angle increased to 92°. Moreover, the inclusion of CA led to a significant decrease in water vapor transmission rate from 863 to 427 ($g/m^2/day$), confirming again the formation of cross-linking. The percentage of weight loss after 30 days was 71.43% (F-CSG/CA), indicating that the prepared biofilm was biodegradable within 45 days. After addition of CA, the network structure increased the thermal stability from 232 to 258 °C. The developed biofilm had promising qualities as a competitive alternative to plastics, including the ease of manufacture, superior strength, and biodegradability. The findings concluded that the synthesized biofilm could be a prominent polymeric material in lieu of synthetic polymers (LDPE, HDPE, PE, and PP) for the manufacture of biodegradable and environmentally friendly polybags.

■ ASSOCIATED CONTENT

Supporting Information

The Supporting Information is available free of charge at https://pubs.acs.org/doi/10.1021/acsomega.4c06400.

https://doi.org/10.1021/acsomega.4c06400
ACS Omega 2025, 10, 8960−8970

Cellulose extraction, preparation of cellulose nanocrystals (CNC), fabrication of biofilm, thermogravimetric analysis, EDX mapping (PDF)

AUTHOR INFORMATION

Corresponding Author

Mosummath Hosna Ara − *Chemistry Discipline, Khulna University, Khulna 9208, Bangladesh*; Email: hosnaara1@gmail.com

Authors

Md. Hafizul Islam − *Department of Chemistry, International University of Business Agriculture and Technology, Dhaka 1230, Bangladesh*

Mubarak A. Khan − *Sonali Bag Research Laboratory, Bangladesh Jute Mills Corporation, Dhaka 1000, Bangladesh*

Jannatul Naime − *Chemistry Discipline, Khulna University, Khulna 9208, Bangladesh*

Md. Abu Rayhan Khan − *Chemistry Discipline, Khulna University, Khulna 9208, Bangladesh*; orcid.org/0000-0002-9719-1266

Md. Latifur Rahman − *Sonali Bag Research Laboratory, Bangladesh Jute Mills Corporation, Dhaka 1000, Bangladesh*

Tania Akter Ruhane − *Sonali Bag Research Laboratory, Bangladesh Jute Mills Corporation, Dhaka 1000, Bangladesh*

Complete contact information is available at: https://pubs.acs.org/10.1021/acsomega.4c06400

Author Contributions

This work was conducted by all authors.

Notes

The authors declare no competing financial interest.

ACKNOWLEDGMENTS

The authors are grateful to Chemistry Discipline, Khulna University, and Sonali Bag Research Laboratory, Bangladesh Jute Mills Corporation, for the laboratory and instrumental support.

REFERENCES

(1) Kumar, A.; Deshmukh, R. K.; Gaikwad, K. K. Quality preservation in banana fruits packed in pine needle and halloysite nanotube-based ethylene gas scavenging paper during storage. *Biomass Convers. Biorefin.* **2024**, *14* (5), 6311−6320.

(2) Xia, Q.; Chen, C.; Yao, Y.; et al. A strong, biodegradable and recyclable lignocellulosic Bioplastic. *Nat. Sustainability* **2021**, *4* (7), 627−635.

(3) Hussain, S.; Akhter, R.; Maktedar, S. S. Advancements in sustainable food packaging: from eco-friendly materials to innovative technologies. *Sustainable Food Technol.* **2024**, *2* (5), 1297−1364.

(4) Chen, Y.; Huang, C.; Miao, Z.; et al. Tailoring Hydronium ion Driven Dissociation-Chemical Cross-Linking for Superfast One-Pot Cellulose Dissolution and Derivatization to Build Robust Cellulose Films. *ACS Nano* **2024**, *18* (12), 8754−8767.

(5) Droguet, B. E.; Liang, H. L.; Frka-Petesic, B.; et al. Large-scale fabrication of structurally coloured cellulose nanocrystal films and effect pigments. *Nat. Mater.* **2022**, *21* (3), 352−358.

(6) Heise, K.; Kontturi, E.; Allahverdiyeva, Y.; et al. Nanocellulose: recent fundamental advances and emerging biological and biomimicking applications. *Adv. Mater.* **2021**, *33* (3), No. 2004349.

(7) Navya, P.; Gayathri, V.; Samanta, D.; et al. Bacterial cellulose: A promising biopolymer with interesting properties and applications. *Int. J. Biol. Macromol.* **2022**, *220*, 435−461.

(8) Azahari, N.; Othman, N.; Ismail, H. Biodegradation studies of polyvinyl alcohol/corn starch blend films in solid and solution media. *J. Phys. Sci.* **2011**, *22* (2), 15−31.

(9) Bruna, A. S. M.; João, H. O. R.; Lindaiá, S. C.; et al. Characterization of cassava starch films plasticized with glycerol and strengthened with nanocellulose from green coconut fibers. *Afr. J. Biotechnol.* **2017**, *16* (28), 1567−1578.

(10) Ramaraj, B. Crosslinked poly (vinyl alcohol) and starch composite films. II. Physicomechanical, thermal properties and swelling studies. *J. Appl. Polym. Sci.* **2007**, *103* (2), 909−916.

(11) Krumova, M.; López, D.; Benavente, R.; et al. Effect of crosslinking on the mechanical and thermal properties of poly (vinyl alcohol). *Polymer* **2000**, *41* (26), 9265−9272.

(12) Ghanbarzadeh, B.; Almasi, H.; Entezami, A. A. Improving the barrier and mechanical properties of corn starch-based edible films: Effect of citric acid and carboxymethyl cellulose. *Ind. Crops Prod.* **2011**, *33* (1), 229−235.

(13) Gunarathne, D. S.; Udugama, I. A.; Jayawardena, S.; et al. Resource recovery from bio-based production processes in developing Asia. *Sustainable Prod. Consumption* **2019**, *17*, 196−214.

(14) Saha, K. K.; Hossain, M.; Ali, M.; et al. Feasibility study of coconut coir dust briquette. *J. Bangladesh Agric. Univ.* **2016**, *12* (2), 369−376.

(15) Hasan, K. M. F.; Horváth, P. G.; Kóczán, Z.; et al. Thermo-mechanical properties of pretreated coir fiber and fibrous chips reinforced multilayered composites. *Sci. Rep.* **2021**, *11* (1), No. 3618.

(16) Siakeng, R.; Jawaid, M.; Asim, M.; et al. Alkali treated coir/pineapple leaf fibres reinforced PLA hybrid composites: Evaluation of mechanical, morphological, thermal and physical properties. *eXPRESS Polym. Lett.* **2020**, *14* (8), 717−730.

(17) Mamani, D. C.; Nole, K. S. O.; Montoya, E. E. C.; et al. Minimizing organic waste generated by pineapple crown: a simple process to obtain cellulose for the preparation of recyclable containers. *Recycling* **2020**, *5* (4), 24.

(18) Hassani, F.-Z. S. A.; Salim, M. H.; Kassab, Z.; et al. Crosslinked starch-coated cellulosic papers as alternative food-packaging materials. *RSC Adv.* **2022**, *12* (14), 8536−8546.

(19) Cerqueira, J. C.; Penha, J. S.; Oliveira, R. S.; et al. Production of biodegradable starch nanocomposites using cellulose nanocrystals extracted from coconut fibers. *Polímeros* **2017**, *27*, 320−329.

(20) de Andrade, M. R.; Nery, T. B. R.; de Santana e Santana, T. I.; et al. Effect of cellulose nanocrystals from different lignocellulosic residues to chitosan/glycerol films. *Polymers* **2019**, *11* (4), 658.

(21) Song, K.; Zhu, X.; Zhu, W.; et al. Preparation and characterization of cellulose nanocrystal extracted from Calotropis procera biomass. *Bioresour. Bioprocess.* **2019**, *6* (1), 45.

(22) Marichelvam, M. K.; Jawaid, M.; Asim, M. Corn and rice starch-based bio-plastics as alternative packaging materials. *Fibers* **2019**, *7* (4), 32.

(23) Rumi, S. S.; Liyanage, S.; Abidi, N. Conversion of low-quality cotton to bioplastics. *Cellulose* **2021**, *28*, 2021−2038.

(24) Wang, H.; et al. Soil burial biodegradation of antimicrobial biodegradable PBAT films. *Polym. Degrad. Stab.* **2015**, *116*, 14−22.

(25) Yongvanich, N. Isolation of nanocellulose from pomelo fruit fibers by chemical treatments. *J. Nat. Fibers* **2015**, *12* (4), 323−331.

(26) Elanthikkal, S.; Gopalakrishnapanicker, U.; Varghese, S.; et al. Cellulose microfibres produced from banana plant wastes: Isolation and characterization. *Carbohydr. Polym.* **2010**, *80* (3), 852−859.

(27) Liu, C.-F.; Ren, J. L.; Xu, F.; et al. Isolation and characterization of cellulose obtained from ultrasonic irradiated sugarcane bagasse. *J. Agric. Food Chem.* **2006**, *54* (16), 5742−5748.

(28) Gao, X.; Chen, K. L.; Zhang, H.; et al. Isolation and characterization of cellulose obtained from bagasse pith by oxygen-containing agents. *BioResources* **2014**, *9* (3), 4094.

(29) Geethamma, V.; Thomas Mathew, K.; Lakshminarayanan, R.; et al. Composite of short coir fibres and natural rubber: effect of chemical modification, loading and orientation of fibre. *Polymer* **1998**, *39* (6−7), 1483−1491.

https://doi.org/10.1021/acsomega.4c06400
ACS Omega 2025, 10, 8960−8970

(30) Kongkaew, P. In *Mechanical Properties of Banana and Coconut Fibers Reinforced Epoxy Polymer Matrix Composites*, International Conference, Tokyo, Japan, 2016.
(31) Reddy, N.; Yang, Y. Citric acid cross-linking of starch films. *Food Chem.* **2010**, *118* (3), 702−711.
(32) Zuraida, A.; et al. The effect of water and citric acid on sago starch bio-plastics. *Int. Food Res. J.* **2012**, *19* (2), 715−719.
(33) Yu, J.; Ning, W.; Xiaofei, M. The effects of citric acid on the properties of thermoplastic starch plasticized by glycerol. *Starch − Stärke* **2005**, *57* (10), 494−504.
(34) Qin, Y.; Wang, W.; Zhang, H.; et al. Effects of citric acid on structures and properties of thermoplastic hydroxypropyl amylomaize starch films. *Materials* **2019**, *12* (9), 1565.
(35) Sharmin, N.; Sone, I.; Walsh, J. L.; et al. Effect of citric acid and plasma activated water on the functional properties of sodium alginate for potential food packaging applications. *Food Packag. Shelf Life* **2021**, *29*, No. 100733.
(36) Sankhla, S.; Sardar, H. H.; Neogi, S. Greener extraction of highly crystalline and thermally stable cellulose micro-fibers from sugarcane bagasse for cellulose nano-fibrils preparation. *Carbohydr. Polym.* **2021**, *251*, No. 117030.
(37) An, V. N.; Nhan, H. T. C.; Tap, T. D.; et al. Extraction of high crystalline nanocellulose from biorenewable sources of Vietnamese agricultural wastes. *J. Polym. Environ.* **2020**, *28*, 1465−1474.
(38) Huang, C.; Gao, Y.; Chen, Y.; et al. Molecular dissociation of DTMS tailoring cellulose regeneration and hydrophobic modification for building highly transparent cellulose films. *J. Cleaner Prod.* **2024**, *451*, No. 142107.
(39) Lu, P.; Hsieh, Y.-L. Preparation and characterization of cellulose nanocrystals from rice straw. *Carbohydr. Polym.* **2012**, *87* (1), 564−573.
(40) Sommer, A.; Staroszczyk, H.; Sinkiewicz, I.; et al. Preparation and characterization of films based on disintegrated bacterial cellulose and montmorillonite. *J. Polym. Environ.* **2021**, *29*, 1526−1541.
(41) Ma, X.; Yu, J.; Kennedy, J. F. Studies on the properties of natural fibers-reinforced thermoplastic starch composites. *Carbohydr. Polym.* **2005**, *62* (1), 19−24.
(42) Thawien, W. Characteristics and properties of rice starch films reinforced with palm pressed fibers. *Int. Food Res. J.* **2010**, *17*, 535−547.
(43) Holland, B. J.; Hay, J. N. Thermal degradation of nylon polymers. *Polym. Int.* **2000**, *49* (9), 943−948.
(44) Alvarez, V.; Vázquez, A. Thermal degradation of cellulose derivatives/starch blends and sisal fibre biocomposites. *Polym. Degrad. Stab.* **2004**, *84* (1), 13−21.
(45) Zhou, X.-Y.; Jia, D. M.; Cui, Y. F.; et al. Kinetics analysis of thermal degradation reaction of PVA and PVA/starch blends. *J. Reinf. Plast. Compos.* **2009**, *28* (22), 2771−2780.
(46) Shi, R.; Zhang, Z.; Liu, Q.; et al. Characterization of citric acid/glycerol co-plasticized thermoplastic starch prepared by melt blending. *Carbohydr. Polym.* **2007**, *69* (4), 748−755.
(47) Lee, H.; You, J.; Jin, H. J.; et al. Chemical and physical reinforcement behavior of dialdehyde nanocellulose in PVA composite film: A comparison of nanofiber and nanocrystal. *Carbohydr. Polym.* **2020**, *232*, No. 115771.
(48) Namphonsane, A.; Suwannachat, P.; Chia, C. H.; et al. Toward a circular bioeconomy: Exploring pineapple stem starch film as a plastic substitute in single use applications. *Membranes* **2023**, *13* (5), 458.
(49) Muhammad, A.; Rashidi, A. R.; Buddin, M. Effect of coconut fiber reinforcement on mechanical properties of corn starch bioplastics. *Int. J. Eng. Technol.* **2018**, *7*, 267−270.
(50) Judawisastra, H.; Sitohang, R.; Marta, L. Water absorption and its effect on the tensile properties of tapioca starch/polyvinyl alcohol bioplastics. *IOP Conf. Ser.: Mater. Sci. Eng.* **2017**, *223*, No. 012066.
(51) Cioica, N.; et al. Water absorption and degradation of packages based on native corn starch with plasticizers. *Stud. Univ. Babes-Bolyai Chem.* **2015**, *60* (1), 45−55.
(52) Gerezgiher, A.; Szabó, T. Crosslinking of starch using citric acid. *J. Phys.: Conf. Ser.* **2022**, *2315*, No. 012036.
(53) Heebthong, K.; Ruttarattanamongkol, K. Physicochemical properties of cross-linked cassava starch prepared using a pilot-scale reactive twin-screw extrusion process (REX). *Starch − Stärke* **2016**, *68* (5−6), 528−540.
(54) Prachayawarakorn, J.; Tamseekhram, J. Chemical modification of biodegradable cassava starch films by natural mono-, di-and tri-carboxylic acids. *Songklanakarin J. Sci. Technol.* **2019**, *41* (2), No. e1.
(55) Vogler, E. A. Structure and reactivity of water at biomaterial surfaces. *Adv. Colloid Interface Sci.* **1998**, *74* (1−3), 69−117.
(56) Yue, H.; Zheng, Y.; Zheng, P.; et al. On the improvement of properties of Bioplastic composites derived from wasted cottonseed protein by rational cross-linking and natural fiber reinforcement. *Green Chem.* **2020**, *22* (24), 8642−8655.
(57) Zhou, J.; Zhang, J.; Ma, Y.; et al. Surface photo-crosslinking of corn starch sheets. *Carbohydr. Polym.* **2008**, *74* (3), 405−410.
(58) Maiti, S.; Ray, D.; Mitra, D. Role of crosslinker on the biodegradation behavior of starch/polyvinylalcohol blend films. *J. Polym. Environ.* **2012**, *20*, 749−759.
(59) Seligra, P. G.; Medina Jaramillo, C.; Famá, L.; et al. Biodegradable and non-retrogradable eco-films based on starch−glycerol with citric acid as crosslinking agent. *Carbohydr. Polym.* **2016**, *138*, 66−74.

https://doi.org/10.1021/acsomega.4c06400
ACS Omega 2025, 10, 8960−8970